

Theory of shape evolution of InAs quantum dots on $\text{In}_{0.5}\text{Ga}_{0.5}\text{As}/\text{InP}(001)$ substrate

Peter Kratzer^{1,5}, Aparna Chakrabarti², Quincy K K Liu³ and Matthias Scheffler⁴

¹ Fachbereich Physik and Center for Nanointegration (CeNIDE), Universität Duisburg-Essen, Lotharstr. 1, D-47048 Duisburg, Germany

² Raja Ramanna Centre for Advanced Technology, Indore 452013, India

³ Abteilung (SF5) Theoretische Physik, Helmholtz-Zentrum-Berlin, Glienicker Strasse 100, D-14109 Berlin, Germany

⁴ Fritz-Haber-Institut der Max-Planck-Gesellschaft, Faradayweg 4-6, D-14195 Berlin, Germany

E-mail: Peter.Kratzer@uni-duisburg-essen.de

New Journal of Physics **11** (2009) 073018 (16pp)

Received 25 February 2009

Published 7 July 2009

Online at <http://www.njp.org/>

doi:10.1088/1367-2630/11/7/073018

Abstract. In this work, the quantum dot (QD) formation of InAs on $\text{In}_{0.5}\text{Ga}_{0.5}\text{As}/\text{InP}(001)$ has been studied theoretically using a hybrid approach. The surface energies were calculated using density functional theory. For elastic relaxation energies, continuum elasticity theory was applied. This hybrid method, as already shown in the literature, takes into account the atomic structure of the various facets of the QDs as well as the wetting layer. Our study deals with the aspect of shape evolution of InAs QDs on a ternary substrate. It shows how the island shape close to equilibrium evolves with varying volume in $\text{InAs}/\text{In}_{0.5}\text{Ga}_{0.5}\text{As}/\text{InP}(001)$ epitaxy. Overall, our study indicates that for this system, there may exist two paths for island growth: one path involves an early energetic stabilization of flat, hut-shaped islands with high-index facets (that may persist due to kinetic limitations), whereas the other path involves islands with larger height-to-base ratios that develop low-index facets. At large volumes, the steeper but more compact islands tend to be energetically more favourable compared to the elongated shapes.

⁵ Author to whom any correspondence should be addressed.

Contents

1. Introduction	2
2. Calculational method	4
3. Results and discussion	6
3.1. Shape evolution of InAs QDs	6
3.2. Stability analysis of hut-shaped islands	12
3.3. Comparison with other materials systems	13
4. Conclusion	14
Acknowledgments	14
References	14

1. Introduction

About two decades ago, spontaneous formation of dislocation-free islands was observed [1]–[3] during the heteroepitaxial growth of strained films of semiconducting materials on lattice-mismatched substrates. These islands, after being overgrown by a capping layer, can be functionalized for the confinement of neutral or charged excitations, and have since been known as quantum dots (QDs). While the islands, from an atomistic point of view, are three dimensional and have a definite size and shape, the QDs are often considered as zero-dimensional systems in semiconductor physics. This is because they confine charge carriers (electrons and/or holes) in all three dimensions of space. Thus having discrete excitation spectra, they are sometimes also called artificial atoms. The confined carriers give rise to novel interesting electronic and optical properties of potential technological relevance. In order to understand and possibly tailor these properties, it is necessary to know about, and control, their size and shape, the three-dimensional composition profile and the strain distribution in the QDs. These structural properties are influenced both by the first step of the growth procedure, the spontaneous formation of free-standing islands on the substrate in Stranski–Krastanov growth mode, and by the second step, overgrowth of these islands by the capping layer. The present study attempts to contribute to a better understanding of the first step, the shape evolution of the free-standing islands, which is a prerequisite for any further studies, e.g. of capping layer growth. The subject of island shape and size evolution turned out to be of considerable interest both for applications, and for a more fundamental understanding of heteroepitaxial growth. A number of studies have been devoted to the thermodynamics [4]–[6] and kinetics [7] of island growth, and the field of island evolution has been found to be rich in interesting physical phenomena. As examples, we refer to early theoretical works [8]–[10] as well as experimental studies of island shape evolution [11]–[15].

On the basis of scanning tunnelling microscopy (STM) studies of free-standing islands of Ge on Si (see e.g. [16]) and of InAs on GaAs (see e.g. [17]), a unified picture of shape evolution has been suggested [18, 19]. In both cases, the experiments found evidence for an evolution from small islands with shallow facets (*pyramids*) to large islands that display a variety of steeper facets (*domes*). While the orientations of island side facets for InAs on $\text{In}_{0.5}\text{Ga}_{0.5}\text{As}/\text{InP}(001)$ are analogous to InAs/GaAs(001), the lattice mismatch $\Delta a = (a_{\text{substrate}} - a_{\text{island}})/a_{\text{island}}$ in the InAs/ $\text{In}_{0.5}\text{Ga}_{0.5}\text{As}/\text{InP}(001)$ system ($\Delta a = -3.2\%$) is much smaller than that for InAs/GaAs ($\Delta a = -6.7\%$), but similar to Ge/Si ($\Delta a = -3.8\%$). For the two heteroepitaxial systems with moderate lattice mismatch, the occurrence of elongated islands has been reported for certain growth conditions. For Ge/Si, these are the so-called hut clusters [2, 20] (islands with a

rectangular base area and a shallow inverted V-shaped roof of pitch of the $\{105\}$ family), while for InAs on InGaAs/InP, elongated QDs with shallow $\{136\}$ or $\{137\}$ facets and a parallelogram-shaped base area have been observed experimentally [21]. In this paper, we propose a general explanation for the occurrence of elongated islands at moderate lattice mismatch, related to the dominant role of surface energy for small QD nuclei. We find this explanation to be more satisfactory than previous ones [21] invoking the elastic energy gain due to relaxation near island edges. Moreover, our study of growth of InAs on a ternary substrate, i.e. $\text{In}_{0.5}\text{Ga}_{0.5}\text{As}/\text{InP}(001)$, could help give the claimed generality [18] of shape evolution a broader empirical basis.

As further motivation for our study, we refer to the technological interest in QD growth in ternary compound semiconductor systems with moderate lattice mismatch. The growth of InAs QDs has been reported on InGaAs/InP [22], InP [21], [23]–[25] and InGaAsP/InP [26]. These substrates allow the growth of larger and less strained QDs compared to the usual GaAs substrate, with the further perspective of fabricating devices that emit light at the wavelengths required for telecommunication. With the same goal, InAs QDs have been grown on a metamorphic InGaAs buffer layer on GaAs that reduces the lattice mismatch. With this growth technique, long-wavelength light emission [27] and lasing [28] at room temperature have been demonstrated. To our knowledge, no material-specific theoretical study has been presented for island evolution on ternary compound substrates so far. While the growth of ternary materials is certainly more complex than elemental or binary semiconductor growth and requires a materials-specific discussion of each system, the present work on InAs islands on $\text{In}_{0.5}\text{Ga}_{0.5}\text{As}$ could help give some general guiding principles for island evolution.

For our present work, we assume that the QDs consist of pure InAs, following a set of previous studies in the literature [4, 29]. The experimental realization that comes closest to the studied situation is the deposition of pure InAs on top of an InGaAs buffer layer grown on InP. There is experimental [30, 31] as well as theoretical [32] evidence that indium atoms tend to segregate to the surface in epitaxy of $\text{In}_x\text{Ga}_{1-x}\text{As}$. Due to the segregation layer, it is unlikely that atomic exchange processes between In adatoms and the topmost substrate layers could lead to intermixing of In with Ga atoms from the substrate. The situation is different from the growth of InAs QDs on GaAs(001), where some interdiffusion of GaAs and InAs has been inferred from the interpretation of x-ray diffraction data [33]. Another situation where large composition gradients in QDs may arise is the simultaneous deposition of In and Ga atoms on GaAs(001) in atomic-layer epitaxy [34]. Henceforth, the term intermixing refers to the phenomenon in which Ga atoms from the substrate are incorporated at In lattice sites of both the wetting layer and the QDs. Whenever an intermixed wetting layer is formed, the relief in elastic energy by QD formation will be less than that for the case of a pure InAs wetting layer. Therefore, our present calculations should be considered as an upper bound for elastic energy relief. While a full theoretical treatment of intermixed QDs is beyond the scope of the present paper, we will qualitatively discuss the effect of intermixing on QD shape evolution in the results section.

This paper is organized as follows: in the section on the calculational method, we briefly explain the hybrid approach [4, 29] to calculate the stability of the islands. In the section on results and discussion, we calculate the shapes of the islands for growth conditions close to equilibrium. The shape evolution with increasing volume of the QDs is investigated. Moreover, conditions for the stability of hut-shaped islands and of the existence of two growth scenarios are discussed. We compare our results with the highly lattice-mismatched case of InAs/GaAs(001) [29]. Finally, we summarize our results in the conclusion section.

2. Calculational method

For the present study, we are mainly interested in the energy gain due to island formation in heteroepitaxy, which is the driving force for the spontaneous formation of QDs. To calculate this quantity, it is not feasible and even not necessary to compute the total energy of an entire QD at the level of *ab initio* calculations, and hence a hybrid approach is the method of choice [4, 29]. The problem can be broken down into two steps as explained here. First, for InAs QDs, the InAs surface energies for several surface orientations are computed within density functional theory (DFT) [35] using knowledge about the atomistic surface structure. Then the elastic relaxation energy of the system is calculated for the case of a low areal density of islands, within continuum elasticity theory, applying the finite-element method (FEM). The total energy gain due to island formation originates from the following terms: (i) strain relaxation in both the island and the substrate and (ii) energy cost due to formation of the island's facets and (iii) edges. Hence we can define the total energy lowered due to island formation, E_{tot} , as follows:

$$E_{\text{tot}} = E_{\text{relax}} + E_{\text{surf}} + E_{\text{edge}}, \quad (1)$$

in which the contributions are from (i) volume relaxation E_{relax} , (ii) surface formation E_{surf} and (iii) edge formation E_{edge} . E_{relax} is the lowering of elastic deformation energy when the material forms an inhomogeneously strained island surrounded by a wetting layer instead of one biaxially strained wetting layer,

$$E_{\text{relax}} = E_{\text{elast}}^{\text{is}} - \epsilon_{\text{film}} V < 0. \quad (2)$$

It is obtained as the difference between the remaining elastic energy $E_{\text{elast}}^{\text{is}}$ in the island relaxed under the epitaxial constraint, and the elastic energy in an equivalent volume V of the uniformly strained homogeneous wetting layer under the same epitaxial constraint, where ϵ_{film} is the strain energy per unit volume of the latter wetting layer. For a large enough QD containing thousands of atoms, the continuum description of elasticity is sufficiently accurate to capture the elastic energy originating from the lattice mismatch. In the present case, this mismatch is -3.2% , and hence the error associated with a linear treatment of the elastic problem as compared to a fully nonlinear treatment is estimated to be less than 5% (cf DFT calculations of biaxially strained films in [36]). Both $E_{\text{elast}}^{\text{is}}$ and ϵ_{film} are obtained from linear elasticity theory, numerically for the island using FEM, analytically for the film. The first-order elastic moduli for InAs and $\text{In}_{0.5}\text{Ga}_{0.5}\text{As}$ are taken from standard experimental literature [37]. The latter represent linear interpolation between the elastic moduli of InAs and GaAs. Their values are $c_{11} = 101.2$ GPa, $c_{44} = 49.5$ GPa and $c_{12} = 50.0$ GPa.

We consider the evolution of the dots as a function of volume through a certain sequence of shapes. For each of these shapes, E_{relax} is calculated using FEM. The FEM calculations were carried out using the commercial programme MARC [38]. Table 1 lists the elastic energy per unit volume, e_{relax} as defined in equation (4), for the different shapes considered in this work.

The surface energy E_{surf} is the cost in energy due to the creation of different facets on the side of the InAs island. This term has been calculated by DFT [35] within the local-density approximation [39] for the exchange-correlation-energy functional. The DFT calculations have been performed with the *fhi98md* code [40] using norm-conserving pseudopotentials of Hamann type, as described by Fuchs and Scheffler [41]. In the calculation of E_{surf} , we take into account surface reconstructions for the various facets of the dots as well as for the wetting layer of InAs on the substrate. The surface energies for reconstructed InAs surfaces of various orientations, including their strain dependence, have already been calculated in [29] for InAs(137) and in [4]

Table 1. Coefficients in equation (5) for the InAs QDs shown in figures 2(a) and (b).

Figure	S0	SI ₁	SI ₂	SI ₃	SII ₁	SII ₂	SII ₃
e_{relax} (meV Å ⁻³)	-0.377	-0.331	-0.330	-0.325	-0.394	-0.432	-0.455
e_{surf} (meV Å ⁻²)	36.9	30.5	30.4	32.6	37.3	44.1	49.0
e_{edge} (meV Å)	287	235	228	231	501	479	469

for the low-index facets. We use these values in the present work. The explicit expression for the term E_{surf} given below contains the difference between the sum of the surface energies of all the side facets and the surface energy of the wetting layer, all weighted by their respective areas,

$$E_{\text{surf}} = \sum_i \gamma^{(i)}(\epsilon^{(i)}) A^{(i)} - \gamma^{(0)} A^{(0)}. \quad (3)$$

Here, $\gamma^{(i)}(\epsilon^{(i)})$ and $A^{(i)}$ are the (strain-dependent) surface energy per unit area and the surface area for the i th facet of the QD. For strain dependence, the two principal components of the strain tensor on the surface, averaged over each facet area, have been taken from the finite-element calculations. For QD growth, moderately arsenic-rich conditions are typical. To simulate such conditions, the arsenic chemical potential μ_{As} has been taken as $\mu_{\text{As(bulk)}} - 0.2$ eV as in [29]. $A^{(0)}$ denotes the QD base area and $\gamma^{(0)}$ is the surface energy per unit area of the wetting layer, excluding the elastic energy contribution to the formation energy of the wetting layer, which has been taken into account already by the term $\epsilon_{\text{film}} V$ in equation (2). The value for $\gamma^{(0)}$, 38.38 meV Å⁻², is obtained from additional DFT calculations for the film formation energy of an epitaxial InAs film on In_{0.5}Ga_{0.5}As/InP(001) as a function of film thickness Θ (number of InAs monolayers). We note that, while calculating $\gamma^{(0)}$ for the InAs wetting layer on the In_{0.5}Ga_{0.5}As substrate, the lattice constant of the substrate is used; hence the wetting layer is under strain. It is found that the DFT results can be well described by a linear function of Θ . Extrapolating this linear relationship to $\Theta = 0$ yields the required value for $\gamma^{(0)}$. It includes the energetic contributions of both the interface between InAs and In_{0.5}Ga_{0.5}As/InP and the free $\beta 2(2 \times 4)$ -reconstructed surface of the InAs film. First-principles electronic structure calculations are the method of choice to obtain these contributions, since they cannot be derived from a classical physics approach (e.g. continuum elasticity theory). The linear dependence of film formation energy on film thickness Θ is a consequence of the relatively small lattice mismatch of $\Delta a = -3.2\%$ in the case of InAs on In_{0.5}Ga_{0.5}As/InP(001), compared with $\Delta a = -6.7\%$ in the case of InAs on GaAs. Therefore, the nonlinear elastic contributions to the surface and interface energy are found to be unimportant in the present case, whereas a clearly nonlinear dependence was found for the InAs wetting layer on GaAs(001) [6].

Finally, E_{edge} in equation (1) is the energy cost for the creation of edges in the island. An exact treatment of this term would require knowledge of the atomic structure of the edges, and hence is beyond the scope of the hybrid approach employed in this study. Instead, we use a reasonable estimate for the size of the edge contribution. Such an approximative treatment is acceptable, as the edge term is anyway unimportant for large islands (the ratio of edge length to facet area tends to zero), while it allows us to have an improved description of intermediate (not very small) islands whose evolution we want to study. Following Ng and Vanderbilt [42],

the edge term consists of two contributions of opposite sign,

$$E_{\text{edge}} = \sum_{\text{all edges}} \beta^{(i)} L^{(i)} - \sum_{\text{base edges}} \frac{(\Delta\sigma^{(i)})^2}{2Y} L^{(i)} \ln \left(\frac{d^{(i)}}{a_{\text{island}}} \right). \quad (4)$$

The first term accounts for the formation energy of edges, including possible contributions due to incomplete unit cells of the facet reconstructions in the presence of an edge. $L^{(i)}$ are the lengths of the edges, and $\beta^{(i)}$ are the corresponding energies per unit length. Lacking more detailed knowledge, we approximate all $\beta^{(i)}$ by $20 \text{ meV } \text{\AA}^{-1}$. The choice of this value is guided by step energies on GaAs(001), for which values of 2 and $12 \text{ meV } \text{\AA}^{-1}$ have been derived from experiment [43]. The second term accounts for the energy gain from additional elastic relaxation near the edges forming the island base, due to the discontinuity of the surface stress, $\Delta\sigma^{(i)}$, between the QD facets and the wetting layer. This term reflects the effect of surface stress (which is not included in standard continuum elasticity theory) on strain fields in the island and substrate. The distances of two parallel base edges, $d^{(i)}$, measured in multiples of the InAs lattice constant a_{island} , and Young's modulus of InAs, $Y = 51.4 \text{ GPa}$, enter into this expression; see [44, 45]. For a numerical estimate, we use a common value of $\Delta\sigma = 50 \text{ meV } \text{\AA}^{-2}$, which is typical for the *differences* of surface stress between different facets found in DFT calculations [4]. This choice is reasonable, as a similar value of $\Delta\sigma = 45 \text{ meV } \text{\AA}^{-2}$ has been employed to estimate the stress discontinuity at the base of Ge islands on Si(001) [46].

The value of E_{tot} is calculated once for a particular size of the QD (volume V), as described above. Then, using the following scaling law, we calculate the E_{tot} for any size.

$$E_{\text{tot}}/V = e_{\text{relax}} + e_{\text{surf}} V^{-1/3} + e_{\text{edge}} V^{-2/3}, \quad (5)$$

where $e_{\text{relax}} = E_{\text{relax}}/V - \epsilon_{\text{film}} < 0$, $e_{\text{surf}} = E_{\text{surf}}/V^{2/3}$ and $e_{\text{edge}} = E_{\text{edge}}/V^{1/3}$. In the last term, the weak logarithmic dependence on the width of the QD base in equation (4) has been replaced by a constant to simplify the evaluation. Numerical values are provided in table 1. Note that the values for e_{edge} which are in the range of $230\text{--}500 \text{ meV } \text{\AA}^{-1}$ are of the same order of magnitude as a previous estimate based on an atomistic model of a pyramidal QD, $e_{\text{edge}} = 172 \text{ meV } \text{\AA}^{-1}$ [47]. For an isolated island to be stable, the total energy-lowered E_{tot} must be negative. This condition is fulfilled if the first term in equation (5) dominates over the sum of the second and third ones. For comparing different materials systems, it is important to note that e_{relax} is proportional to the second power of the lattice mismatch. Hence the relative importance of the first two terms in equation (5), having opposite sign, is different for InAs QDs on $\text{In}_{0.5}\text{Ga}_{0.5}\text{As}/\text{InP}$ substrate compared to GaAs substrate.

3. Results and discussion

3.1. Shape evolution of InAs QDs

This section deals with the change of shapes of InAs islands with the increase in size (volume), specifically under conditions close to thermodynamic equilibrium. Experimentally, this can be realized by using molecular beam epitaxy (MBE) at growth temperatures that are sufficiently high, such that possible kinetic limitations are not crucial. Then the QD shape is governed by the interplay between elastic energies and surface energies, and its stability can be calculated from the hybrid approach.

In order to identify the main tendencies in island growth, we consider two growth scenarios of how the islands could possibly evolve out of a starting structure. Each scenario is specified

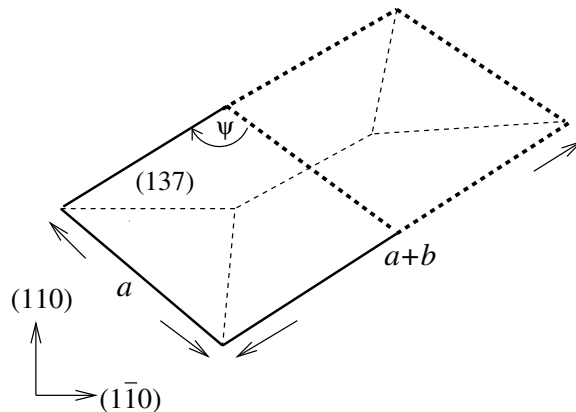


Figure 1. Elongated InAs QD structure shown schematically in top view. The symmetric rhombic base (full lines) is elongated into a parallelogram (thick dashed lines). The thin dashed lines indicate the edges outside the basal plane. For the numerical calculations, the structures in figures 2(a) and (b) have been used.

by a sequence of island shapes. In constructing either sequence, it has been assumed that once some material forms part of the QD, it is incorporated permanently and cannot be re-distributed to augment the shape any further during growth. The starting structure has a flat pyramidal shape with $\{137\}$ side facets, as is observed in STM on InAs QDs on GaAs substrate [13, 29]. Atomic force microscopy and transmission electron microscopy experiments [21, 22] carried out on InAs QDs grown on InGaAs/InP substrate find pyramids bounded by similar high-index facets (labelled $\{136\}$ facets in these works). Additional evidence for $\{137\}$ orientation has been provided from the analysis of chevrons in RHEED patterns [48]. Recently, the ambiguity between the (very close) facet orientations $\{136\}$ and $\{137\}$ has been ascribed to variations in growth rate and annealing temperature [49]. For $\{137\}$ facets, a low-energy surface reconstruction is known, in contrast to the $\{136\}$ facets, where no structural model has been proposed. Therefore $\{137\}$ facets have been used to construct the starting shape (S0 in figures 2(a) and (b)), together with small $(\bar{1}11)$ and $(1\bar{1}1)$ facets that cut the sharp edges.

Experimental studies [21, 22, 25] have found that small islands formed by the growth of InAs on InGaAs/InP often have an elongated shape. The island base has the shape of a parallelogram (cf figure 1). Compared to a mirror symmetric, rhombic base, one pair of edges is elongated. However, each of the two possibilities for the elongation direction occurs with equal probability, arguing against crystallographic asymmetry as a possible explanation. Motivated by these experimental findings, in *growth scenario I* it is assumed that the islands grow in length, keeping the slope of their side facets constant. Alternatively, in *growth scenario II*, the islands grow both in base area and in height, thereby developing steeper side facets, corresponding to low-index surface orientations. This second scenario has been adopted from a previous theoretical study on InAs/GaAs island evolution [29]. In the present work, the InAs islands on InGaAs/InP(001) are investigated along similar lines to probe possible similarities in island evolution on both substrates.

The elongated shapes characteristic of growth scenario I, constructed after taking a cue from the literature [21, 22], are shown in figure 2(a) from top to bottom. The top-most starting structure, S0, has already been described above. Here we assume that it initially grows by filling

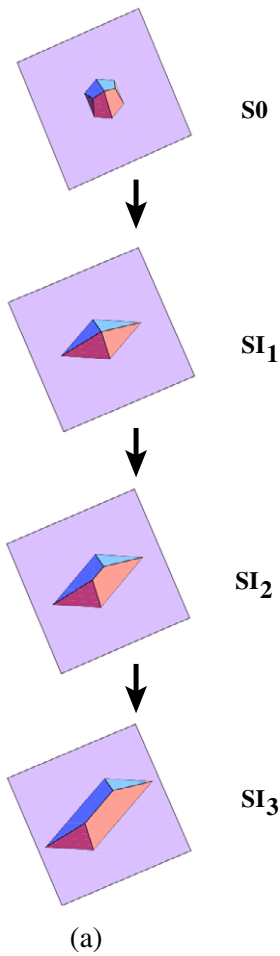
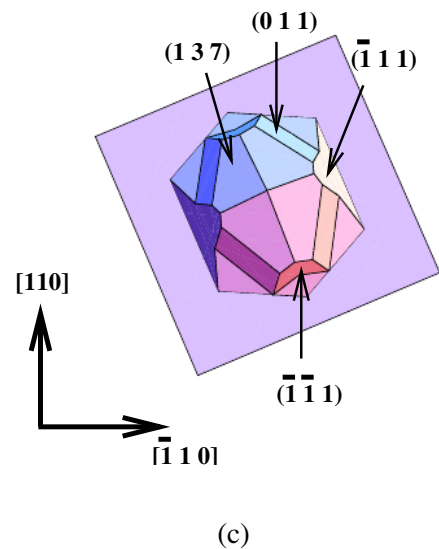
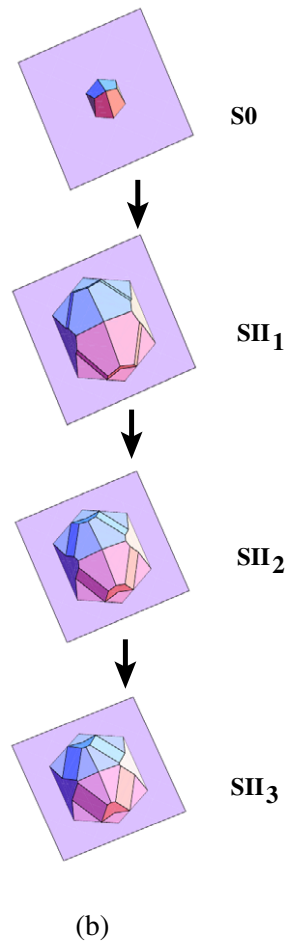
Growth scenario I**Growth scenario II**

Figure 2. (a) *Growth Scenario I*: On top, pyramidal shape predominantly bound by $\{137\}$ facets (S_0), followed by rhombus shape (SI_1), further followed by elongated dot structures, with (a) moderate (shape SI_2) and (b) large elongation (shape SI_3). (b) *Growth Scenario II*: Sequence of shapes considered in searching for energetically stable shapes as a function of volume. On top, pyramidal shape predominantly bound by $\{137\}$ facets (S_0). In shapes SII_1 through SII_3 , low-index facets start appearing in the mid part of the dots. These shapes show the diminishing area of the $\{137\}$ facet at the top. For further details, see text and also [29]. (c) Details of the microfacets of shape SII_2 .

up the cut edges. The dot shapes developing in this way, named after their base areas, are the rhombus dot (SI_1 in figure 2(a)) and the parallelogram dots (SI_2 and SI_3 in figure 2(a)) [22]. The difference between SI_2 and SI_3 is the extent of elongation of the base, which is larger in the latter case. The elongated structures are completely bounded by side facets from the $\{137\}$ high-index family.

The non-elongated structures considered in growth scenario II, having C_{2v} symmetry, are shown in figure 2(b). This growth scenario has a sequence of shapes that runs from simple pyramids to complex domes with higher aspect ratios (from 0.20 for S_0 to 0.22 for SII_1 , 0.25

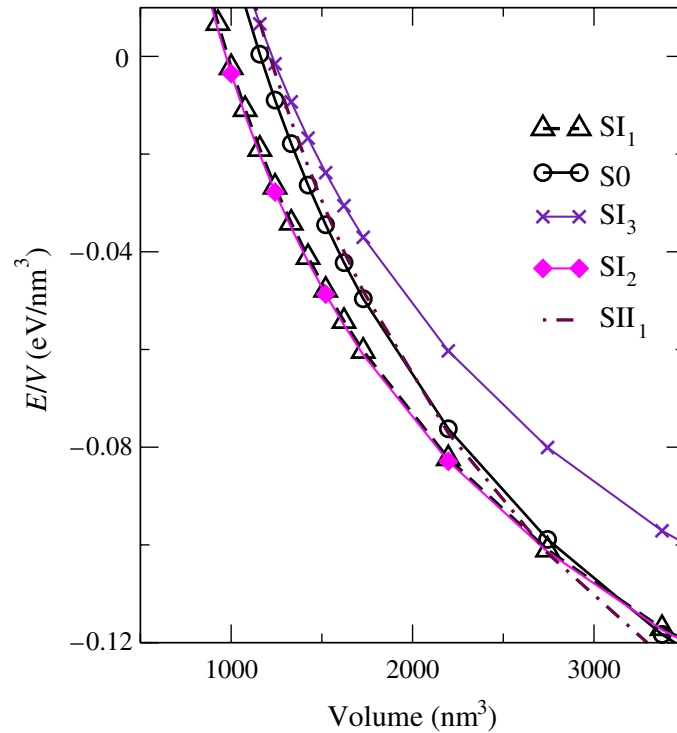


Figure 3. Energy gain per volume for the formation of QDs of different shapes, as shown in figure 2, as a function of dot volume up to 3500 nm^3 . The moderately elongated structure SI_2 (cf figure 2(a)) is signified by the solid line with the filled diamond symbol; the largely elongated structure SI_3 (cf figure 2(a)) is signified by the solid line with the cross symbol; shape SI_1 (cf figure 2(a)) is signified by the long dashed line with the empty triangle up symbol; shape S_0 (cf figure 2(a)) is signified by the solid line with the empty circle symbol; shape SII_1 (cf figure 2(b)) is signified by the dot-dashed line.

for SII_2 and 0.29 for SII_3). This is achieved by continuously adding more and more of the steep (011), (101), (0 $\bar{1}$ 1) and ($\bar{1}$ 01) facets between the upper and lower part of the island (see structure SII_2 in figure 2(c) for details of the facets). The proposed shape of the domes, with {137} facets in both their lower and upper parts, is consistent with the thermodynamic requirement that whenever shallow facets with low surface energy appear as part of the equilibrium shape, they must appear at both the top and the bottom of the QDs [50]. A similar sequence of shapes has been employed to analyse the growth of InAs QDs on GaAs, guided by STM data [29].

The results of our calculations using the hybrid approach are presented in figures 3 and 4, where the energy gain per volume for the formation of QDs of different shapes is given as a function of QD volume, for a small and a large volume range, respectively. The energetically most favourable shape changes with increase in the QD volume. Figure 3 addresses the regime of small QD nuclei. For a volume up to about 1000 nm^3 , the energy balance expressed by E_{tot}/V is positive for all the shapes considered (figures 2(a) and (b)). The positive value indicates that these nuclei are only metastable compared to a homogeneous wetting layer. We find a range of volumes (up to about 2700 nm^3) where the moderately elongated dot (cf SI_2 in figure 2(a)) is energetically the most stable shape. This is because the surface contribution, E_{surf}/V , tends to

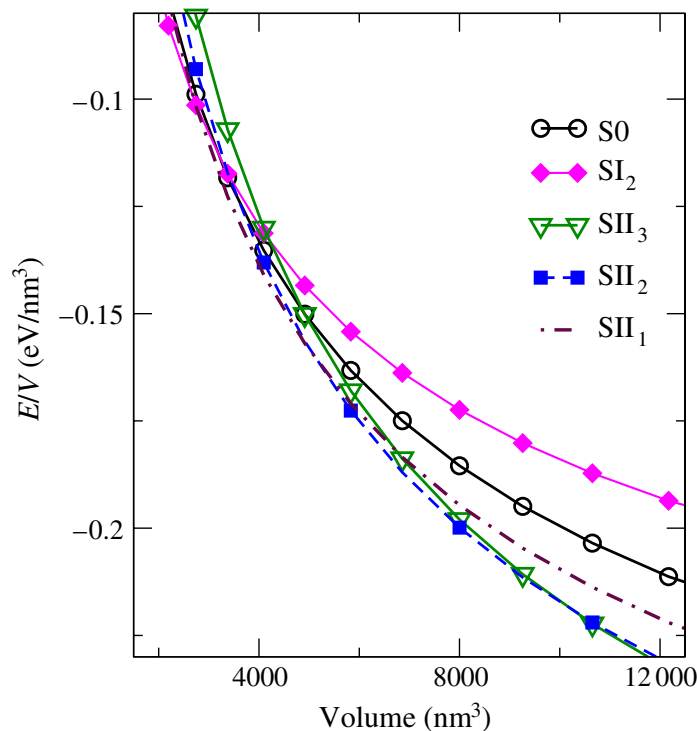


Figure 4. Energy gain per volume for the formation of QDs of different shapes, as shown in figure 2, as a function of dot volume, for larger volume, up to 12 500 nm³. Shapes S0, SI₂ and SII₁ are signified by the same line and symbols, as in figure 3. Shapes SII₂ and SII₃ (cf figure 2(b)) are signified by the dashed line with the filled square symbol and the solid line with the empty triangle down symbol, respectively. It is observed that different shapes are being stabilized with increasing volume. The elongated shape SI₂ is stabilized at lower volumes. Shapes SII₁ and SII₂ are the stable shapes in the typical experimental volume range.

lower the total energy in case of the elongated structure, since the surface-to-volume ratio for an elongated dot structure is more favourable, as will be explained in section 3.2. It is interesting to observe that up to about 3000 nm³ volume, the energy gain for the rhombus dots (SI₁) is very close to the elongated structure SI₂. (The two curves are indistinguishable in figure 3.) Beyond that volume, the energy gain of the former is higher, but their energies are still very close. This observation conforms with the experimental findings by Michon *et al* [21] and Hwang *et al* [22]. They observe that the QDs mostly look elongated, as is observed in case of some III–V QD systems [22, 51]. Some QDs of rhombus shape, similar to SI₁, are also present in these experiments. Hence it is the growth scenario I proposed in figure 2(a) that matches with the experimental results of Michon *et al* [21] and Hwang *et al* [22].

In figure 4, we display the results of the higher volume regime. Beyond a volume of about 2700 nm³, flat pyramid-type islands (SII₁ in figure 2(b)), mainly bounded by {137} facets but already with some {011} microfacets present (see, for reference, shape SII₂ in figure 2(c) for identification of these microfacets), energetically overcome the elongated shape, as already evident in figure 3. After the volume of the growing QD has reached about 5000 nm³, the shape

gradually changes from SII_1 to SII_2 (figure 2(b)), i.e. the low-index facets now make up a larger fraction of the total island surface. Above a volume of about $10\,000\text{ nm}^3$, another shape (SII_3 in figure 2(b)) appears to be most stable. A fully developed dome shape, i.e. the shrinking of the shallow $\{137\}$ facets at the top of the QD, as has been observed in the case of InAs QDs on GaAs substrate [29], is found to be *not* energetically preferable according to our analysis in case of InAs/InGaAs/InP, even in the large volume limit. Based on MBE growth experiments of III–V QDs at high temperatures, Saito *et al* [12] pointed out that rather symmetric shapes are preferred under these conditions. This observation is consistent with growth scenario II shown in figure 2(b), where the evolution runs through symmetric shapes with an increasing fraction of low-index, high-symmetry facets. In further support of growth scenario II, we should mention that the signature of parallelogram dots undergoing a shape transition to dots with higher-symmetry facets has been observed by Hwang *et al* [22], as some of their parallelogram dots display a small fraction of $\{011\}$ facets.

In summary, our calculations suggest that the growth of InAs QDs on InGaAs initially proceeds along growth scenario I, i.e. by elongation of the islands, but may later switch to growth scenario II. It appears plausible that, for large volumes, the islands will start to grow in height and develop steeper side facets, as this allows for the upper part of the island to relax its elastic energy more efficiently. Given that the relief of strain energy is the main driving force for the evolution of large islands, symmetric islands will eventually be energetically favoured over elongated ones, since a compact, symmetric shape allows a maximum of strain energy relief while keeping the concomitant increase of the surface area minimal. We note that a switching from growth scenario I to growth scenario II very likely requires the re-distribution of material that has already been incorporated in an (elongated) island, which is possible only at sufficiently high temperatures. Whether the switching actually occurs or not may thus depend on growth conditions, in particular, on the closeness to thermodynamic equilibrium. It needs to be mentioned here that both Michon *et al* [21] and Hwang *et al* [22] grow their samples using metal-organic vapour deposition (MOCVD), a technique where the concentration of surface species is typically rather far from thermodynamic equilibrium conditions. Hence it is conceivable that islands obtained by this growth technique may have taken the following path. Once initial energetic stabilization of the elongated structures has taken place, growth proceeds by filling preferentially the smaller of the side facets, driving the islands to even more elongated shapes, even beyond the point where these shapes are energetically most stable. Such an amplification of a pre-existing asymmetry due to kinetic limitations has already been suggested to explain the occurrence of elongated hut clusters in Ge/Si epitaxy [20, 52].

We briefly discuss the changes to be expected if intermixing of In and Ga species occurs in the wetting layer and in the interior and basal parts of the QDs [33]. As InAs has lower surface energy than GaAs, both the QD surface and the wetting layer surface will be very indium-rich due to surface segregation, and hence our estimate of the surface energy contribution will be practically unchanged also in case of bulk intermixing. However, if intermixing is accounted for, the system starts already in a less strained state before QD formation, and the energy gain $|e_{\text{relax}}|$ will be smaller. In fact, e_{relax} scales as Δa^2 , where Δa is the relative lattice mismatch between pure InAs and the average lattice constant of the intermixed wetting layer material (as calculated e.g. from Vegard's law). This implies that the asymptotic values of E/V approached by the curves in figures 3 and 4 for large volumes V will be smaller (less negative) under conditions where intermixing is important. With the plausible assumption that intermixing (which mainly takes place in the basal regions of the QD) is equally important for all shapes, the cross-over

between growth scenario I and scenario II will take place at even larger QD volumes in the case of intermixed systems.

3.2. Stability analysis of hut-shaped islands

It is remarkable that elongated QDs have been reported for Ge/Si(001) and InAs/In_{0.5}Ga_{0.5}As/InP, i.e. materials systems with moderate lattice mismatch, but not for a highly mismatched system such as InAs/GaAs. In order to understand the reason for the difference, it is interesting to further analyse the stability criteria of elongated islands within the framework of the hybrid approach. For both materials systems, the occurrence of hut-shaped islands is closely related to the existence of a high-index facet with low surface energy. For InAs, the {137} surface has a low surface energy, as demonstrated by recent DFT calculations [29]. For Ge on Si(001), a similar role is played by the {105} facets of Ge [53, 54]. Since hut-shaped islands with these facet orientations are rather shallow, their ability to relieve strain is very limited. In addition, the coefficient e_{relax} is proportional to the square of the lattice mismatch. For both reasons, the second term is found to dominate over the first term in equation (5) at low QD volumes, where the QDs are metastable compared to the wetting layer. As we shall explain below, some elongation of the islands is energetically favourable under these conditions encountered in low-mismatch systems.

To be specific, let us consider the island in figure 1 with base lengths a and $a + b$ of the two edges. The elongation is described by the parameter $x = b/a$, which is zero for symmetrical islands and positive otherwise. The larger of the two angles enclosed by the base edges is called ψ . For the Ge/Si hut clusters with rectangular base, $\psi = 90^\circ$, while $\psi = 126.86^\circ$ for InAs islands with {137} facets. The facet angle ϕ is defined as the angle between the normal vectors of the QD side facet and the substrate plane. It is $\phi = 11.31^\circ$ for the {105} facets of GeSi islands, and $\phi = 24.31^\circ$ for the {137} facets of InAs islands. In equation (3), we have $A^{(0)} = a(a + b)\sin\psi$, and four side facets with an overall area $A^{(1)} = a(a + b)\sin\psi/\cos\phi$. Hence, we obtain

$$E_{\text{surf}} = a^2(1 + x)(\gamma^{(1)}/\cos\phi - \gamma^{(0)})\sin\psi. \quad (6)$$

Inserting the DFT values of the surface energy, $\gamma^{(0)} = 38.4 \text{ meV } \text{\AA}^{-2}$ and $\gamma^{(1)} = 39.5 \text{ meV } \text{\AA}^{-2}$, yields $E_{\text{surf}} = 4.0 a^2(1 + x) \text{ meV } \text{\AA}^{-2}$ for the specific case of InAs islands on In_{0.5}Ga_{0.5}As/InP. The volume of such an island is calculated to be $V = \frac{1}{6}a^3(1 + \frac{3}{2}x)\sin^2\psi\tan\phi$. Thus, the second term in equation (5), E_{surf}/V , is proportional to $(1 + x)/(1 + \frac{3}{2}x)$, i.e. it is a decreasing function of x . Since the surface energy term is positive, a finite x helps to lower the total energy cost (per unit volume or per particle) associated with QD formation. For small, shallow islands, the elastic relaxation energy, i.e. the first term in equation (5), is smaller than the two other contributions, and only weakly dependent on the elongation parameter x . In the case of InAs/In_{0.5}Ga_{0.5}As/InP, while for the symmetric island SI₁ (in figure 2(a)) we obtain $e_{\text{relax}} = -0.331 \text{ meV } \text{\AA}^{-3}$, for the two elongated islands displayed in figure 2(a) (SI₂, SI₃) our FEM calculation yields values of $e_{\text{relax}} = -0.330 \text{ meV } \text{\AA}^{-3}$ and $-0.325 \text{ meV } \text{\AA}^{-3}$, respectively. Thus, the elastic energy is found to be a weakly increasing function of x . We note that our conclusions remain true also in the case of intermixing, as the elastic energy term will be smaller (and even less dependent on x) due to the reduced average lattice mismatch in intermixed systems. The edge energy contribution is the smallest of the three terms in equation (5), showing the same trend as the surface contribution, and does not affect the conclusions. The most favourable island shape is eventually

determined by a balance between the energy gain from elastic relaxation and the energy cost of forming the side facets and edges. For small islands, the surface term acts in favour of some elongation, whereas for larger islands, the elastic relaxation energy becomes more important, and hence compact, symmetrical islands with $x = 0$ become the energetically preferable island shape.

Our finding that the tendency to form elongated QDs is mainly a result of savings in the energetic cost of forming side facets contrasts the proposed explanation of Michon *et al* [21], who invoked elastic contributions. Their argument follows an idea originally worked out by Tersoff and Tromp [8], who showed that elastic energy relaxation at a flat, quasi-two-dimensional island of constant height favours elongation. In the work of Michon *et al* [21], constrained minimization of the total energy (rather than E_{tot}/V , as in our study) with respect to one of the lateral dimensions of the island leads to an energy-minimizing elongated shape. However, the authors remark that the elongated QDs do *not* correspond to an *absolute* minimum of the energy and therefore the anisotropy of the QD shape would *not* result from a full minimization of the energy of the system without any constraint. In their approach, minimizing the energy with respect to *all* dimensions leads to an optimal shape that is symmetric [21], consistent with our results for large islands whose shape is dominated by strain relief.

3.3. Comparison with other materials systems

According to our results, the optimum shape of the QDs depends on their size. Hence it is important to know which QD sizes are achieved experimentally. The maximum size is determined by the onset of dislocation formation. Beyond this size, part of the strain energy relief is inelastic, and the present theory is no longer applicable. In this subsection, we compare the size and shape of the QDs for InAs/GaAs, InAs/InGaAs/InP and Ge/Si for the ranges of volumes observed experimentally. Free-standing InAs QDs grown on GaAs are reported with a volume of up to 1000 nm^3 , and the QDs in this volume range are observed to have a fully developed dome shape [29]. Experimental reports about the volume range of InAs QDs on InGaAs or InP are rather scarce. Michon *et al* [21] speak about volumes between 600 and 3000 nm^3 . Parry *et al* [25] report an average lateral dimension of about $50\text{--}60 \text{ nm}$ and a maximum height of about 4 nm , which results in a volume larger than 6000 nm^3 . For GeSi QD on Si(001), a system with similar lattice mismatch, the QD volume is reported [55] to be at least 1000 nm^3 . For the Ge/Si system, large QDs with volumes up to about $10\,000 \text{ nm}^3$ have been reported by Costantini *et al* [19]. Hence, for the typical experimental volume range of the InAs/InGaAs/InP QDs, from about 1000 nm^3 to about $10\,000 \text{ nm}^3$, shapes SI₁ and SI₂ shown in figure 2(a) and shapes SII₁ and SII₂ shown in figure 2(b) are expected to be stable according to this study. The extremely large volume required to observe the transition to shape SII₃ of figure 2(b) predicted from the present calculations is unlikely to be reached in practical experiments. Similarly, shape SI₃ of figure 2(a) is not expected to be observed experimentally.

We have discussed in great detail in [29] the shape evolution for InAs QDs on GaAs substrate. From what we have presented here, it is clear that the results in the cases of two substrates, namely GaAs and InGaAs, are quite different. Unlike the InAs/GaAs system, but similar to Ge/Si, we observe the possibility of the formation of elongated islands on the latter substrate.

4. Conclusion

The observation of elongated QDs for InAs on $\text{In}_{0.5}\text{Ga}_{0.5}\text{As}$ or InP substrates, but not for InAs QDs on GaAs, calls for a theoretical explanation. In the present work, we probe the shape evolution as a function of QD volume in the case of InAs QDs on the $\text{In}_{0.5}\text{Ga}_{0.5}\text{As}/\text{InP}(001)$ substrate and have conjectured about the existence of two growth scenarios. A hybrid approach has been used for this study, where the elastic energy change associated with QD formation is calculated using elasticity theory, while the surface energies of the QD facets are taken from DFT calculations using the atomic structure of these surfaces as input. For small QDs, the calculations show that somewhat elongated QDs are more stable than the more symmetric ones. Under growth conditions away from equilibrium, this anisotropy may be amplified due to kinetic limitations during growth, and experimental observations of the elongated, asymmetric dots, grown by MOCVD, can be explained thus. Close to thermodynamic equilibrium and at larger volumes (beyond 2700 nm^3), however, non-elongated islands are expected to be energetically favourable over elongated ones. While the present study deals with energetics alone, and thus cannot help identify the precise nature of the kinetic limitations in growth, it corroborates the prevailing view in the literature that some element of kinetics must be involved in the appearance of elongated QDs (also called hut clusters) in moderately mismatched heteroepitaxy. Moreover, the implications of intermixing of In and Ga in the QDs for the above findings are briefly discussed.

Acknowledgments

We thank Volkswagen Stiftung for funding the joint Indo-German project, under which this work was carried out. A C and P K acknowledge the hospitality of JNCASR, Bangalore, which enabled us to exchange ideas. A C thanks K C Rustagi, S M Oak and V C Sahni for encouragement and support as well as S R Barman, V K Dixit, S Pal, C Kamal and S D Singh for fruitful discussions.

References

- [1] Eaglesham D J and Cerullo M 1990 *Phys. Rev. Lett.* **64** 1943
- [2] Mo Y-W, Savage D E, Swartzentruber B S and Lagally M G 1990 *Phys. Rev. Lett.* **65** 1020
- [3] Guha S, Madhukar A and Rajkumar K C 1990 *Appl. Phys. Lett.* **57** 2110
- [4] Moll N, Kley A, Pehlke E and Scheffler M 1996 *Phys. Rev. B* **54** 8844
Pehlke E, Moll N, Kley A and Scheffler M 1997 *Appl. Phys. A* **65** 525
Moll N, Scheffler M and Pehlke E 1998 *Phys. Rev. B* **58** 4566
- [5] Liu Q K K, Moll N, Scheffler M and Pehlke E 1999 *Phys. Rev. B* **60** 17008
- [6] Wang L G, Kratzer P, Scheffler M and Moll N 1999 *Phys. Rev. Lett.* **82** 4042
Wang L G, Kratzer P, Moll N and Scheffler M 2000 *Phys. Rev. B* **62** 1897
- [7] Carlsson N, Seifert W, Petersson A, Castrillo P, Pistol M E and Samuelson L 1994 *Appl. Phys. Lett.* **65** 3093
Dobbs H T, Vvedensky D D, Zangwill A, Johansson J, Carlsson N and Seifert W 1997 *Phys. Rev. Lett.* **79** 897
- [8] Tersoff J and Tromp R M 1993 *Phys. Rev. Lett.* **70** 2782
- [9] Daruka I, Tersoff J and Barabasi A L 1999 *Phys. Rev. Lett.* **82** 2753
- [10] Daruka I and Tersoff J 2002 *Phys. Rev. B* **66** 132104
- [11] Schmidbauer M, Hatami F, Hanke M, Schäfer P, Braune K, Masselink W T, Köhler R and Ramsteiner M 2002 *Phys. Rev. B* **65** 125320

- [12] Saito H, Nishi K and Sugou S 1999 *Appl. Phys. Lett.* **74** 1224
- [13] Marquez J, Geelhaar L and Jacobi K 2001 *Appl. Phys. Lett.* **78** 2309
- [14] Xu M C, Temko Y, Suzuki T and Jacobi K 2005 *Phys. Rev. B* **71** 075314
- [15] Ngo C Y, Yoon S F, Fan W J and Chua S J 2006 *Phys. Rev. B* **74** 245331
- [16] Montalenti F *et al* 2004 *Phys. Rev. Lett.* **93** 216102
- [17] Xu M C, Temko Y, Suzuki T and Jacobi K 2005 *J. Appl. Phys.* **98** 083525
- [18] Costantini G, Rastelli A, Manzano C, Songmuang R, Schmidt O G, Kern K and von Kaenel H 2004 *Appl. Phys. Lett.* **85** 5673
- [19] Costantini G, Rastelli A, Manzano C, Acosta-Diaz P, Katsaros G, Songmuang R, Schmidt O G, von Kaenel H and Kern K 2005 *J. Cryst. Growth* **278** 38
- [20] Kästner M and Voigtländer B 1999 *Phys. Rev. Lett.* **82** 2745
- [21] Michon A, Sagnes I, Patriarche G, Beaudoin G, Merat-Combes M N and Saint-Girons G 2006 *Phys. Rev. B* **73** 16532
- [22] Hwang H, Yoon S, Kwon H, Yoon E, Kim H-S, Lee J Y and Cho B 2004 *Appl. Phys. Lett.* **85** 6383
- [23] Ponchet A, Le Corre A, L'Haridon H, Lambert B and Salaün S 1995 *Appl. Phys. Lett.* **67** 1850
- [24] Borgstrom M, Samuelson L, Seifert W, Mikkelsen A, Ouattara L and Lundgren E 2003 *Appl. Phys. Lett.* **83** 4830
- [25] Parry H J, Ashwin M J, Neave J H and Jones T S 2005 *J. Cryst. Growth* **278** 131
- [26] Kawaguchi K, Ekawa M, Kuramata A, Akiyama T, Ebe H, Sugawara M and Arakawa Y 2004 *Appl. Phys. Lett.* **85** 4331
- [27] Seravalli L, Minelli M, Frigeri P, Franchi S, Guizetti G, Patrini M, Ciabattini T and Geddo M 2007 *J. Appl. Phys.* **101** 024313
- [28] Zhukov A E *et al* 2003 *Semiconductors* **37** 1411
- [29] Kratzer P, Liu Q K K, Acosta-Diaz P, Manzano C, Costantini G, Songmuang R, Rastelli A, Schmidt O G and Kern K 2006 *Phys. Rev. B* **73** 205347
- [30] Dehaese O, Wallart X and Mollot F 1995 *Appl. Phys. Lett.* **66** 52
- [31] Rosenauer A, Gerthsen D, Van Dyck D, Arzberger M, Böhm G and Abstreiter G 2001 *Phys. Rev. B* **64** 245334
- [32] Chakrabarti A, Kratzer P and Scheffler M 2006 *Phys. Rev. B* **74** 245328
- [33] Kegel I, Metzger T H, Lorke A, Peisl J, Stangl J, Bauer G, Garcia J M and Petroff P M 2000 *Phys. Rev. Lett.* **85** 1694
- Kegel I, Metzger T H, Lorke A, Peisl J, Stangl J, Bauer G, Nordlund K, Schoenfeld W V and Petroff P M 2001 *Phys. Rev. B* **63** 035318
- [34] Liu N, Tersoff J, Baklenov O, Holmes A L and Shih K C 2000 *Phys. Rev. Lett.* **84** 334
- [35] Hohenberg P and Kohn W 1964 *Phys. Rev.* **136** B864
- Kohn W and Sham L J 1965 *Phys. Rev.* **140** A1133
- [36] Hammerschmidt T, Kratzer P and Scheffler M 2007 *Phys. Rev. B* **75** 235328
- [37] Hellwege K-H 1982 *Physics of Group IV Elements and III-V Elements (Landolt-Börnstein, New Series, Group III, vol 17, Part a)* (Berlin: Springer)
- [38] *MARC User's Guide* 1996 (Palo Alto: MARC Analyses Research Corporation)
- [39] Ceperley D M and Alder B J 1980 *Phys. Rev. Lett.* **45** 566
- Perdew J P and Zunger A 1981 *Phys. Rev. B* **23** 5048
- [40] Bockstedte M, Kley A, Neugebauer J and Scheffler M 1997 *Comput. Phys. Commun.* **107** 187
- [41] Fuchs M and Scheffler M 1999 *Comput. Phys. Commun.* **116** 1
- [42] Ng K and Vanderbilt D 1995 *Phys. Rev. B* **52** 2177
- [43] Heller E J, Zhang Z Y and Lagally M 1993 *Phys. Rev. Lett.* **71** 743
- [44] Shchukin V 1999 *Rev. Mod. Phys.* **71** 1125
- [45] Marchenko V I 1981 *JETP Lett.* **33** 381
- [46] Lu G-H and Liu F 2005 *Phys. Rev. Lett.* **94** 176103
- [47] Hammerschmidt T, Kratzer P and Scheffler M 2008 *Phys. Rev. B* **77** 235303

- [48] Feltron A and Freundlich A 2007 *J. Cryst. Growth* **301–2** 38
- [49] Placidi E, Della Pia A and Arciprete F 2009 *Appl. Phys. Lett.* **94** 021901
- [50] Daruka I and Tersoff J 2002 *Phys. Rev. B* **66** 132104
- [51] Mirin R P, Ibbetson J P, Nishi K, Gossard A C and Bowers J E 1995 *Appl. Phys. Lett.* **67** 3795
- [52] Jesson D E, Chen G, Chen K M and Pennycook S J 1998 *Phys. Rev. Lett.* **80** 5156
- [53] Raiteri P, Migas D B, Miglio L, Rastelli A and von Känel H 2002 *Phys. Rev. Lett.* **88** 256103
- [54] Shklyaev O E, Beck M J, Asta M, Miksis M J and Voorhees P W 2005 *Phys. Rev. Lett.* **94** 176102
- [55] Ross F M, Tersoff J and Tromp R M 1998 *Phys. Rev. Lett.* **80** 984